C31C-1362: Melt Pond and Lead Detection in Melting Ice using ICESat-2 Altimetry and Very-High-Resolution (VHR) Aerial Imagery

Dong Chen[1*], Sinéad L. Farrell[1], Kyle Duncan[2], Jaemin Eun[1], Ellen M. Buckley[3], Michelle A. Hofton[1], Bryan Blair[4], Kutalmis Saylam[5]
1 Dept. of Geographical Sciences, University of Maryland, College Park, United States. 2 ESSIC, University of Maryland, College Park, United States.
3 Brown University, Providence, RI, United States. 4 NASA Goddard Space Flight Center, Code 61A, Greenbelt, MD, United States. 5 The University of Texas at Austin, Austin, Texas, United States.
*Corresponding author. Email: itscd@umd.edu

1. Introduction

ICESat-2 is transforming our ability to measure the evolution of complex sea ice topography, providing a novel remote sensing capability in all seasons. Our goal is to investigate ICESat-2's capabilities to measure sea ice freeboard and thickness as well as melt pond conditions (fraction and depth) during the summer melt season. A region in the central Arctic, north of Greenland was surveyed by a NASA aircraft in July 2022 (**Figure 1**). During the NASA ICESat-2 Summer Sea Ice Campaign 2022, high-resolution lidar data were collected below ICESat-2, by the Land, Vegetation, and Ice Sensor (LVIS) and the Leica Chiroptera. Both systems also collected co-located high-resolution imagery (**Table 1**). We analyze LVIS PhaseOne Georeferenced Imagery (**Figure 2**) and Chiroptera multispectral RGB-NIR imagery (**Figure 3**) to quantify melt characteristics in the study region. A random forest classification scheme applied to the imagery distinguishes open water, sea ice, and melt ponds to derive melt pond fraction in the study area (**Figure 4**). Integrating the image classifications with altimetry data, we examine sea ice freeboard from the LVIS laser altimeter and compare this with data derived from ICESat-2 (**Figure 5**).

2. Study Area

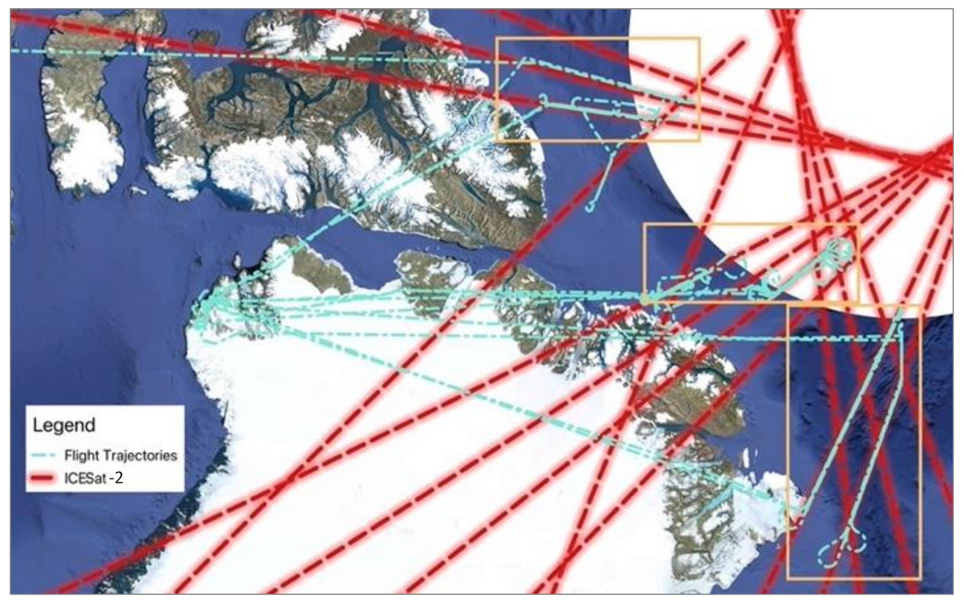

Figure 1. (left) G-V flight survey lines (cyan) and ICESat-2 orbits (red) during the NASA ICESat-2 Summer Sea Ice Campaign 2022 in a survey region north the Lincoln Sea. (**below**) Distribution of the LVIS (blue) and Chiroptera (green) images analyzed in this study. Each dot corresponds to the center of a single image.

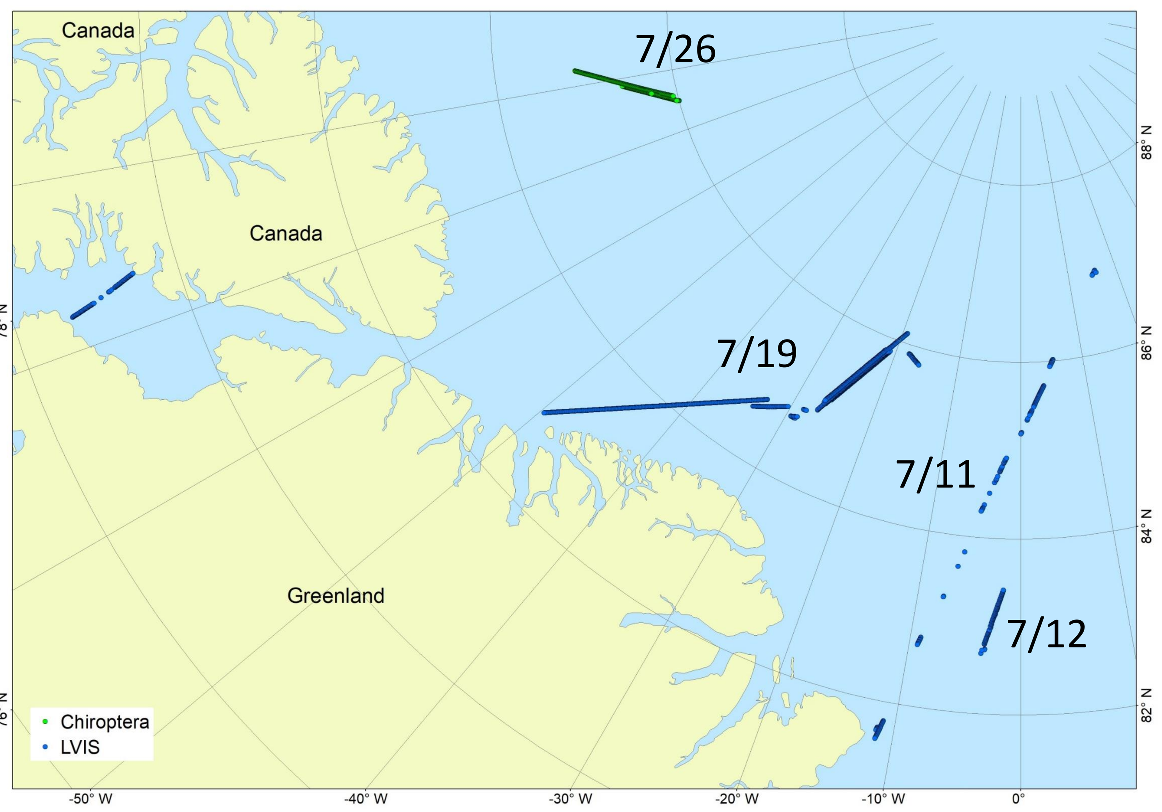

3. Datasets

Table 1. Characteristics of remote sensing data collected during the NASA ICESat-2 Summer Sea Ice Campaign 2022

Platform	Sensor	Technique	Wavelength	Altitude	Swath Width (across track)	Footprint Diameter / Pixel Resolution
Satellite ICESat-2	ATLAS	Laser	532 nm	496 km	6.6 km	~11 m
Aircraft	LVIS	Laser Altimetry	1064 nm	~10 km	~2 km	~8 m
Gulfstream V	LVIS PhaseOne	Optical Imager	Visible Band (RGB)	~10 km	~3 km	0.39 m - 0.50 m
Aircraft	Leica Chiroptera	Bathymetric Lidar	515 nm	~0.5 km	~380 m	~1.5 m
Gulfstream V		Topographic Lidar	1064 nm			
	Chiroptera RCD-30 Camera	Hyperspectral Imager	Visible-NIR Bands (RGB-NIR)	~0.5 km		0.05 m hi-res / 0.50 m lo-res

Data Sources

LVIS lidar: https://nasaext.app.box.com/s/l0f8tfd6gy60bncuev5e4rpj4j8mkjem
LVIS imagery: https://nsidc.org/data/is2olvis1bcv/versions/1
ATL10: https://nsidc.org/data/atl10/versions/6
Chiroptera: https://utexas.box.com/s/476v9jghzioirc3wwbftfnngfegsp4qd

4. Image Classification

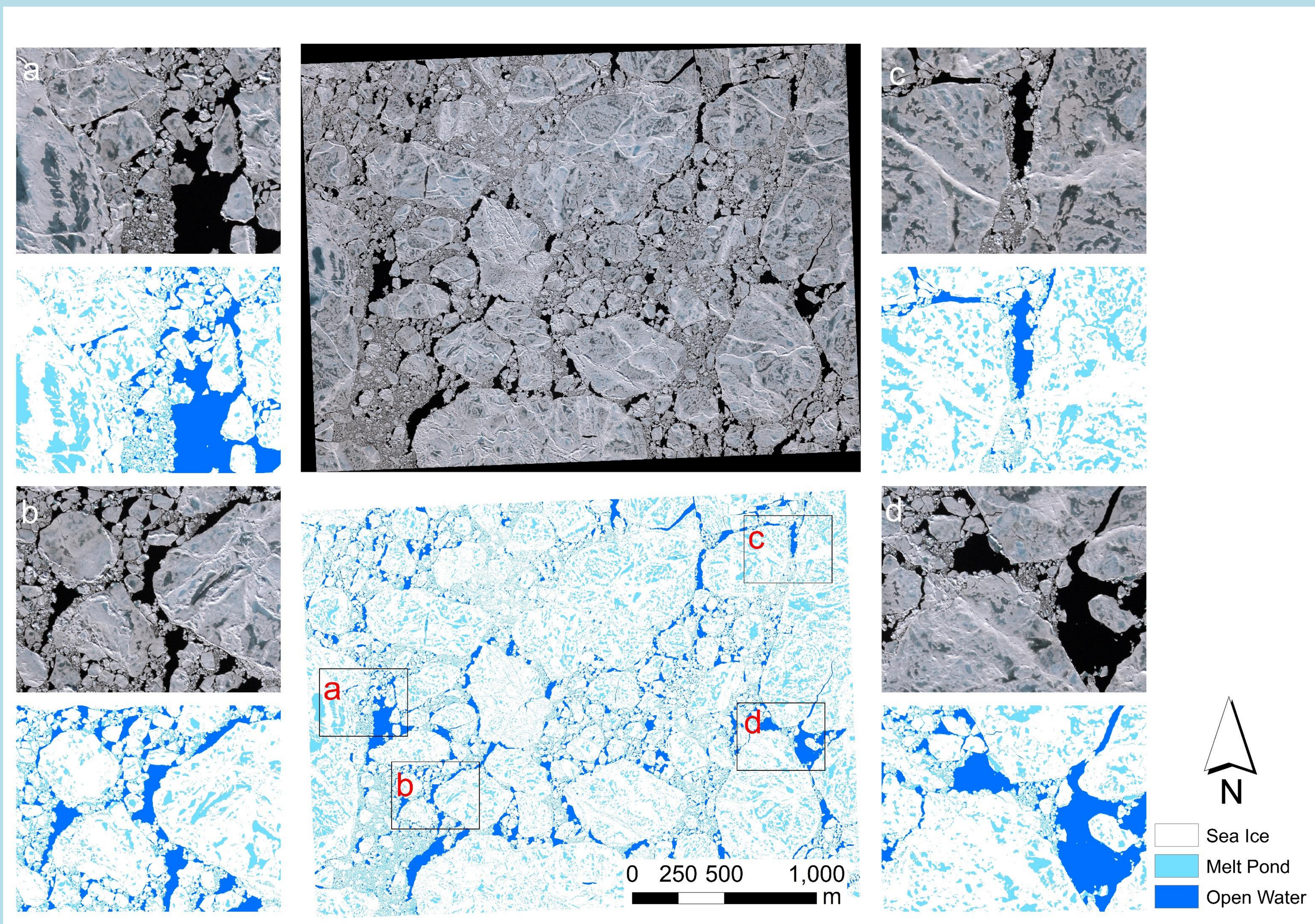

Figure 2. Example classified LVIS image (center) in comparison with the original image (center top). Insets (a) to (d) show zoomed-in views that reveal details of the sea ice (white), melt ponds (cyan) and open water (blue).

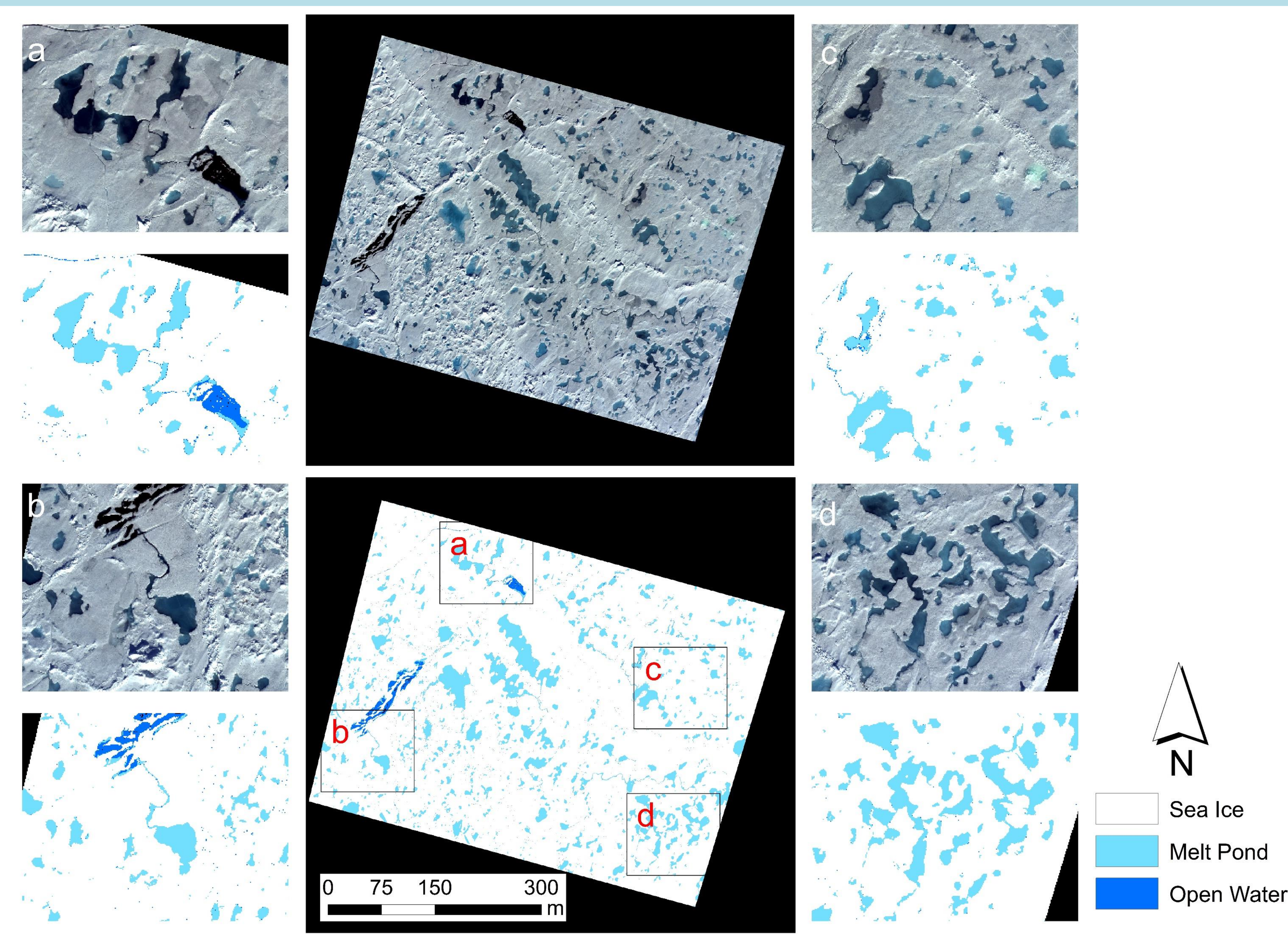

Figure 3. Example classified Chiroptera image (center bottom) in comparison with the original image (center top). Insets (a) to (d) show the zoomed-in views with more details of melt ponds (cyan) on sea ice.

Table 2. Accuracy assessment of the classified LVIS images. Statistics were calculated based on 2,000 randomly-generated points, distributed across 20 images. Reference classification (ground truth) was assigned by an analyst who was not involved in the image classification process. The bottom right value (highlighted in blue) is the overall accuracy.

		Reference				
		Ice	Open Water	Melt Pond	Total	Commission Error
Classified	Ice	971	70	59	1100	11.7%
	Open Water	83	356	61	500	28.8%
	Melt Pond	7	17	376	400	6.0%
	Total	1061	443	496	2000	
	Omission Error	8.5%	19.6%	24.2%		85.2%

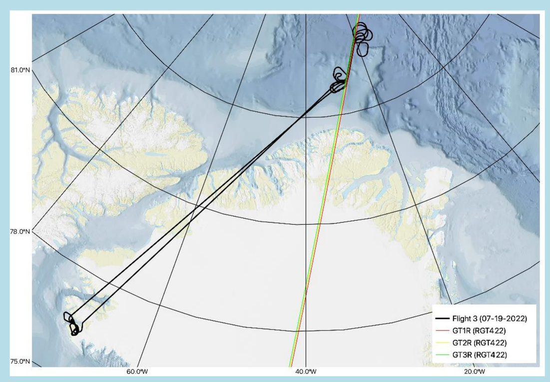

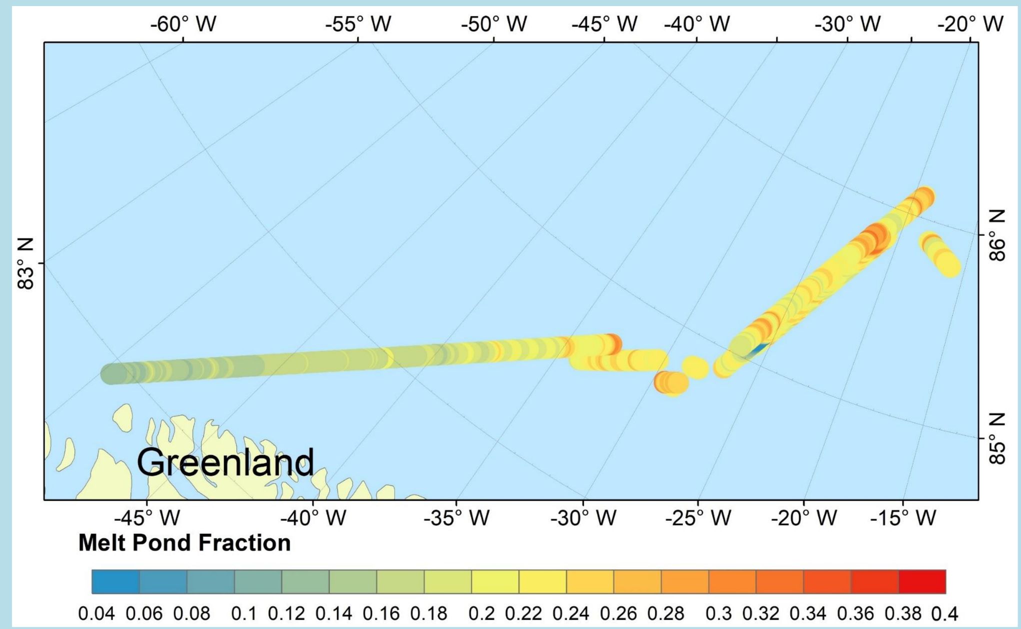

Figure 4. (Top) Survey over sea ice on July 19 2022 beneath a spatiotemporally coincident ICESat-2 orbit (RGT422). (**Right**) Variations in melt pond fraction (%) calculated from classified LVIS images. At the time of the survey, pond fractions were largest in the northeastern sector of the survey line at 20 – 34 %.

5. Integration with Altimetry Data

Sea ice elevation derived from ICESat-2 ATL03 photon heights in the survey area on July 19, 2022 revealing leads and ridges.

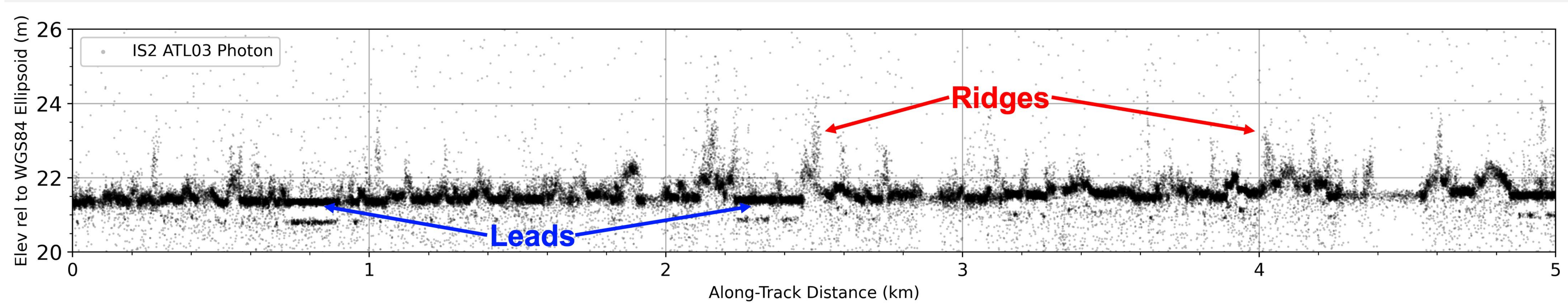

The combination of LVIS data and co-located high-resolution optical imagery (Figure 5a) allows summer sea ice melt characteristics to be quantified in the survey region. The classification of LVIS PhaseOne imagery (Figure 5b) into ice, melt ponds and open water enables each LVIS lidar return to be classified (Figure 5c). Classified LVIS elevations are used to calculate elevation distributions and statistics for each separate surface type (Figure 5d). Modal open water elevation is subtracted from sea ice height to calculate the total freeboard per image (eqn. 1). Elevation distributions and total freeboard (Figure 5e) are derived for the ~120 km transect on July 19 2022 and compared with ICESat-2 ATL10 freeboard estimates collected ~30 minutes prior (Figure 5f). The classified LVIS elevations allow for a direct evaluation of the accuracy of the coincident ICESat-2 data and the sea ice surface-type classification scheme. Improvements in surface type classification will allow for more accurate freeboard heights and sea ice thickness estimates during the summer months.

$$fb_{LVIS} = h - h_{OW} \quad [1]$$

fb_{LVIS}: LVIS freeboard
h : LVIS sea ice height
h_{OW} : open water height

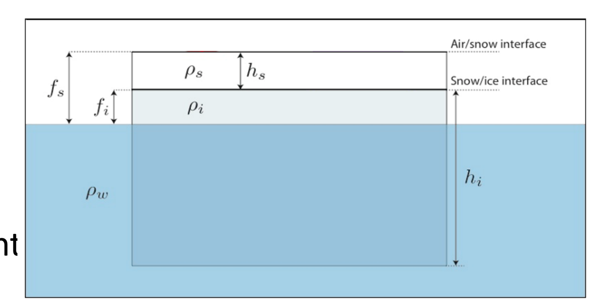

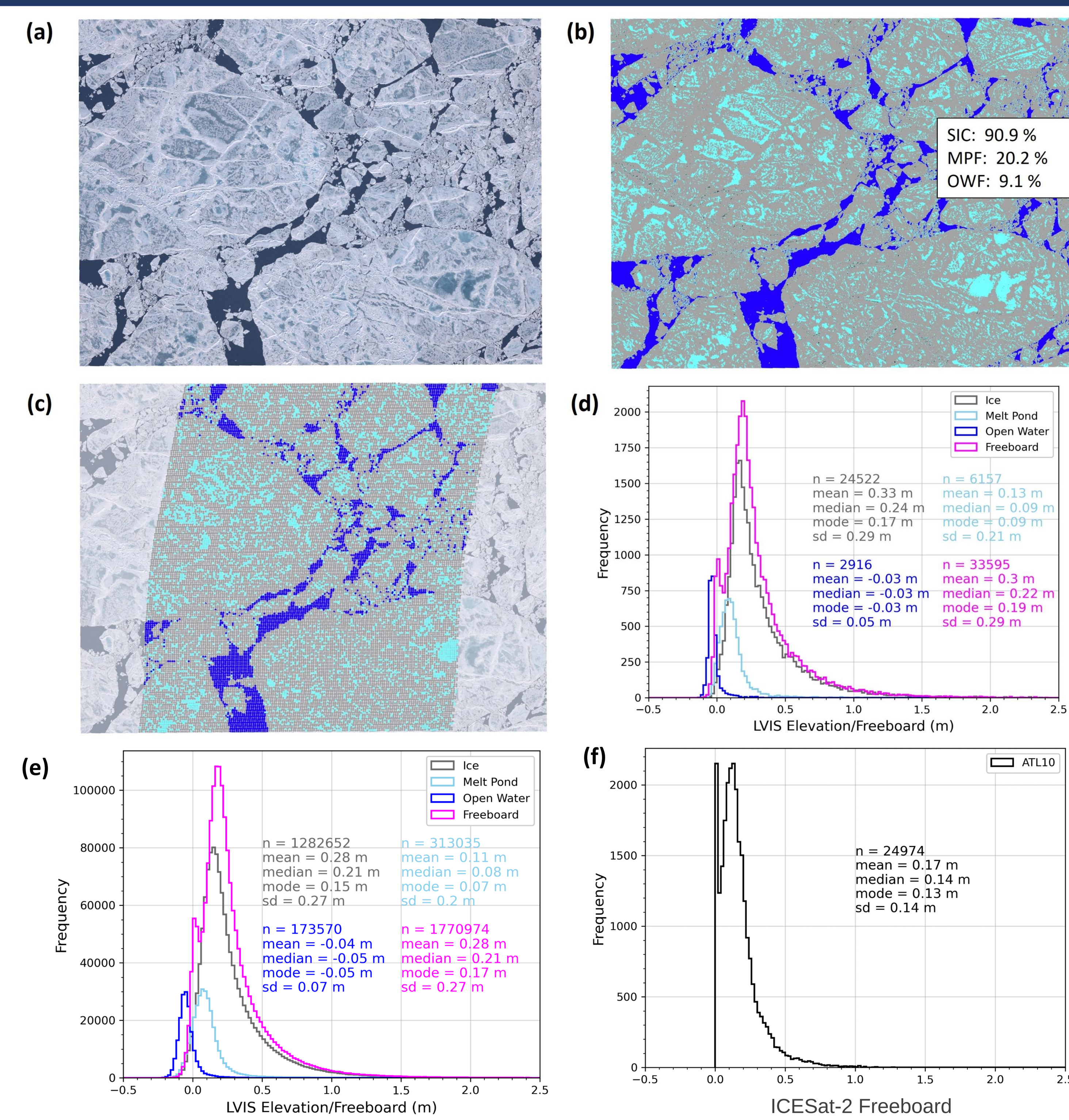

Figure 5. (a) Example of LVIS PhaseOne optical imagery acquired on July 19, 2022. (b) Image in (a) classified into ice (gray), melt ponds (cyan) and open water (blue) with the associated sea ice concentration (SIC), melt pond fraction (MPF) and open water fraction (OWF). (c) Classification of coincident LVIS lidar data using the results from (b). (d) Classified LVIS elevation distributions (bins of 2 cm) and statistics for ice, melt ponds, and open water. Total freeboard (magenta) is the height of the sea ice above the sea surface (including any snow). Freeboard (fb) is derived by subtracting the modal elevation of open water (h_{ow}) from the sea ice height (h) as shown in equation [1]. (e) Same as in (d) but for an entire ~120 km transect acquired on July 19, 2022. (f) ATL10 freeboard along the same transect as in (e). LVIS freeboard is skewed by ice deformation features (i.e., ridges).

Acknowledgments

Our project "Enhancing Laser altimeter Elevation measurements through Validation of Arctic summer sea ice as Temperatures Evolve (ELEVATE)" is supported under NASA GSFC award 80NSSC22K0815. We acknowledge the diligent efforts of Rachel Tilling (NASA GSFC/UMD) and Nathan Kurtz (NASA GSFC) that led to a successful field campaign. We also thank the NASA G-V and ICESat-2 instrument teams for processing data used here.